



Deposited via The University of York.

White Rose Research Online URL for this paper:

<https://eprints.whiterose.ac.uk/id/eprint/155643/>

Version: Accepted Version

Article:

Juan-Colás, José, Jung, Yong, Johnson, Steven D et al. (2019) A complicated relationship: Glycosylation, Ca(II), and primary sequence affect the interactions and kinetics between two model mollusk shell intracrystalline nacre proteins. *Biochemistry*. ISSN: 1520-4995

<https://doi.org/10.1021/acs.biochem.9b00867>

Reuse

Items deposited in White Rose Research Online are protected by copyright, with all rights reserved unless indicated otherwise. They may be downloaded and/or printed for private study, or other acts as permitted by national copyright laws. The publisher or other rights holders may allow further reproduction and re-use of the full text version. This is indicated by the licence information on the White Rose Research Online record for the item.

Takedown

If you consider content in White Rose Research Online to be in breach of UK law, please notify us by emailing eprints@whiterose.ac.uk including the URL of the record and the reason for the withdrawal request.

A complicated relationship: Glycosylation, Ca(II), and primary sequence affect the interactions and kinetics between two model mollusk shell intracrystalline nacre proteins.

Jose Juan-Colas,¹ Yong Seob Jung,² Steven Johnson,¹ and John Spencer Evans^{2*}

¹Department of Electronic Engineering, University of York, Heslington, York, YO105DD, United Kingdom.

²Laboratory for Chemical Physics, Center for Skeletal and Craniofacial Biology, New York University, 345 E. 24th Street, NY, NY, 10010 USA.

KEYWORDS: *Pacific red abalone, biomineralization, AP7, AP24, QCM-D, glycosylation, flow cell cytometry*

Supporting Information Placeholder

ABSTRACT: The formation of the mollusk shell requires the participation of proteins, many of which may be interactive with one another. We examined a model protein pair system from the mollusk *Haliotis rufescens* wherein we probed the interactions between recombinant forms of two major nacre layer proteins, AP7, and the glycoprotein, AP24. Here, the focus was on the impact that AP24 glycosylation and primary sequence had on AP24-AP7 binding. We find that both the glycosylated and non-glycosylated variants of AP24 bound to AP7 but with different quantities, kinetics, and internal rearrangements. Moreover, the binding of AP7 with non-glycosylated and glycosylated AP24 was found to be Ca(II) dependent and independent, respectively. Yet both variants of AP24 combine with AP7 to form hybrid hydrogel particles that are similar in their physical properties. Thus, AP7 and AP24 protein sequences are interactive and form hydrogels, but the interactions are tuned by glycosylation and Ca(II). These features may have an impact on nacre matrix formation.

Molluscan shells and pearls are fascinating examples of high performance organic/inorganic biocomposite materials. Although the organic components represent only about 2% weight of the mollusk shell,¹ they provide nanoscale precision

of control over shell fabrication and are responsible for the tremendous enhancement of the strength and elasticity of the material as compared to mineral alone. The fracture toughness of red abalone nacre is about 3000 times higher than the value for pure aragonite,¹ and toughening mechanisms deduced from the crack propagation behavior in nacre are attributed to the structural relationship between the organic macromolecules and inorganic crystals.¹

We now know that protein families play an important role in the mechanical properties of nacre.²⁻⁴ One class of proteins that contributes to nacre toughness are the intracrystalline proteins.²⁻⁶ These proteins are excreted by the mantle epithelial cells and it has been hypothesized that these proteins form hydrogels during the mineral formation process, eventually becoming incorporated into the nacre tablets as organic nano-inclusions which create nanoporosities within nacre tablets and increase the ductility or elasticity of these crystals.⁷⁻¹⁶

There is now great interest in understanding the mechanisms by which intracrystalline proteins control nacre tablet formation and nanoporosity. In the Pacific red abalone, *Haliotis rufescens*, four intracrystalline nacre proteins, AP7, AP24 (a glycoprotein), AP8 α , and AP8 β , have been identified,^{17,18} but only AP7 (AA = 66; MW = 7.5 kDa; pI = 5.43) and AP24 (AA =

146; MW = 24 kDa; pI = 5.53) have been sequenced and studied in detail (Figure S1, Supporting Information).¹⁷ One of the more intriguing findings regarding AP7 and AP24 was the recovery of AP7 - AP24 complexes during nacre extraction protocols, and, the enhanced blocking effects that this protein complex had on the *in vitro* calcite nucleation process.¹⁷ This suggests that there are specific interactions between both proteins within the nacre matrix which may be important not only for inhibiting calcite and promoting the aragonite mineralization process but also the formation of gel nanoinclusions within nacre tablets themselves.⁷⁻¹⁶ However, the details of the interactions between both proteins has yet to be established.

In this Communication we investigated the interactions between recombinant forms of AP7 (rAP7)¹⁵ and AP24 (rAP24G, insect cell expressed, glycosylated; rAP24NG, bacteria expressed, unglycosylated)¹³ to confirm if both protein sequences are interactive and if so, whether the interactions between both proteins rely on the recognition of either the glycan groups or the primary sequence of rAP24 by rAP7. rAP7, rAP24G, and rAP24NG have been demonstrated to self-assemble under mineralization conditions and act as strong calcite blockers *in vitro*.^{13,15} Interestingly, rAP24 is a hybrid N-, O-linked glycoprotein (Supporting Information) that possesses significant levels of anionic monosaccharides (i.e., carboxylate-, sulfate-modified monosaccharides)¹³ which would be expected to contribute significantly to the anionic charge of this protein sequence. We find that in the absence of Ca(II) both rAP24 variants interact with rAP7 via a 2-stage kinetic mechanism but exhibit differences in kinetics. Furthermore, we observe that rAP24NG - rAP7 sequence interactions are 1:1, highly dependent upon Ca(II), and induce conformational change in rAP24NG. In contrast, rAP24G - rAP7 interactions are Ca(II)-independent and do not induce conformational change in rAP24G. Interestingly, we note that both rAP7 - rAP24G and rAP7 - rAP24NG sample mixtures in the presence of Ca(II) result in the formation of hydrogel particles with similar physical properties. Thus, our model recombinant studies indicate that the interaction of AP24 with AP7 is a complicated one: it is affected not only by Ca(II) but also by glycosylation and primary sequence interactivity as well, and these factors most likely are important for nacre matrix formation.

The primary sequences of *in vitro* expressed rAP24NG (bacterial) and rAP24G (insect cell) model proteins are identical, with the only difference being the presence of N- and O-linked glycans on the rAP24G insect cell variant.¹³ Therefore, a screening of each recombinant AP24 protein against the rAP7 protein will measure contribution of insect cell glycosylation and primary sequence on AP7 - AP24 polypeptide interactions. We executed these investigations at pH 8.0 since this is the relevant pH of the *in vitro* calcium carbonate mineralization assays conducted on these proteins,⁷⁻¹⁶ with the actual *in situ* pH of the nacre matrix not known at present. To measure protein-protein interactions we employed QCM-D (quartz crystal microbalance with dissipation) methodology (Figure 1) similar to the *in vitro* studies conducted with other biomineralization proteins.^{7,9,19} Each experiment involved the initial creation of a layer of adsorbed rAP7 protein on poly(L-lysine) using a 500 nM rAP7 solution in 10 mM HEPES buffer pH 8.0 (Figure 1). Subsequent to this step we next introduced either rAP24G or rAP24NG (500 nM each), both dissolved in either the HEPES buffer or in 10 mM CaCl₂ solution in HEPES buffer over the

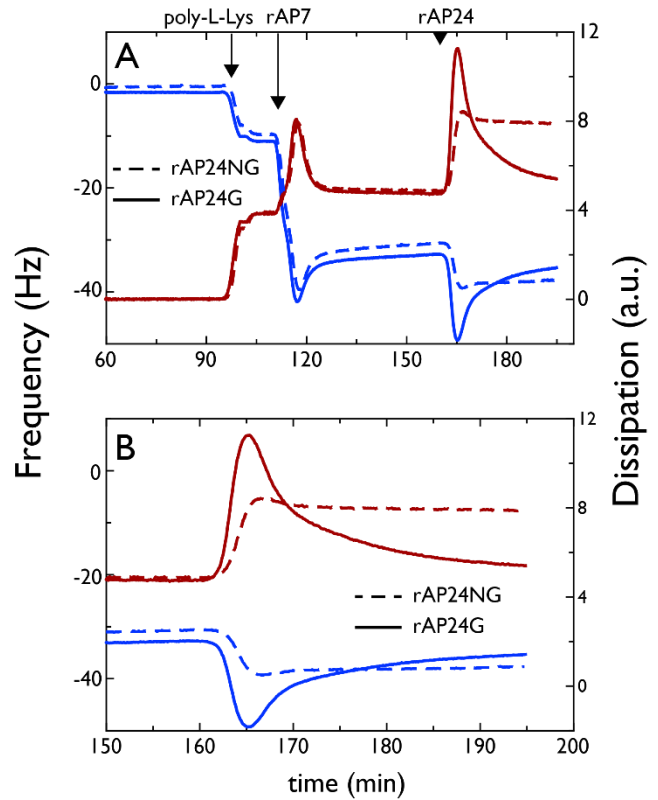


Figure 1. (A) QCM-D experiments of immobilized rAP7 (500 nM in 10 mM HEPES pH 8.0) exposed to either 500 nM rAP24G (solid lines) or 500 nM rAP24NG (dashed lines) in 10 mM CaCl₂ 10 mM HEPES, pH 8.0. Plots show the third harmonic frequency (F3, blue) and dissipation (D3, red) observed under each scenario. The time-dependent introduction is noted on the plots by arrows. These experiments were repeated and found to be reproducible. (B) Enlargement of the QCM-D plot of (A) showing the binding response of each rAP24 protein to the adsorbed rAP7 layer.

immobilized rAP7 layer.

In the presence of Ca(II) (Figure 1), the introduction of 500 nM rAP24NG to the immobilized 500 nM rAP7 layer results in a decrease in resonant frequency, f , accompanied by an increase in dissipation, D , both of which rapidly saturate and remain constant with time. This response is indicative of association between rAP24NG and the immobilized rAP7. In contrast, exposure to 500 nM rAP24G results in an initial and rapid decrease in f , corresponding to an increase in mass due to association of rAP24G. The frequency shift is 40% larger than observed for rAP24NG, indicating a larger mass of rAP24G initially adsorbed onto the rAP7 layer and in contrast to rAP24NG, the frequency then subsequently decreases slowly, almost reaching its initial level after 30 minutes. This confirms that glycosylation of AP24 positively impacts AP24 - AP7 interactions. We note that during this recovery phase the sensor surface remains exposed to the rAP24G solution and the apparent reduction in frequency is thus unlikely to be due to dissociation of rAP24G from the immobilized rAP7. This two-stage kinetic response in f is also observed in the dissipation data (Figure 1) which increase rapidly, before slowly reducing almost back to the initial level. Parallel experiments were also performed in the absence of Ca(II), where a similar two-stage kinetic association curve was observed for both rAP24G and rAP24NG (Figure S2, Supporting

Information), confirming that binding between rAP24G and rAP7 is strongly Ca(II)-dependent.

We analyzed in more detail the protein concentration-dependent interactions of both rAP24 variants, this time starting with a higher concentration of immobilized rAP7 (5 μ M) in the presence of Ca(II) (Figure 2). As we approach the 1:1 molar threshold we note the interactions between rAP7, rAP24G, and

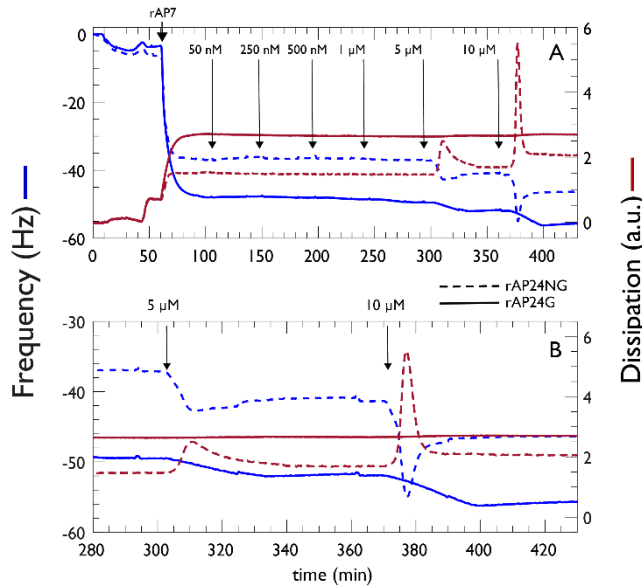


Figure 2 (A) QCM-D experiment of immobilized 5 μ M rAP7 exposed to increasing concentrations of either rAP24G (solid lines) or rAP24NG (dashed lines) in 10 mM CaCl₂, 10 mM HEPES, pH 8.0. (B) Inset of (A) for 5 and 10 μ M of both rAP24N and rAP24NG.

rAP24NG exhibit typical single-stage kinetic binding. In contrast, at a rAP24NG solution concentration above 5 μ M (i.e., > 1:1 molar), we again observe the two-stage kinetic binding between rAP24NG and surface immobilized rAP7. This is not observed for rAP24G. It is worth noting that rAP24NG – rAP7 molecular interactions become significant at a 1:1 molar ratio, which suggests that the two protein sequences form a 1:1 molar ratio complex (see Supplementary Information, Figure S2). Interestingly, dimerization was postulated to occur between native AP7 and AP24 within the nacre.¹⁷ Thus, the AP24 polypeptide sequence recognizes and binds to the AP7 sequence in a 1:1 molecular ratio.

The prominent peaks in frequency and dissipation followed by slow recovery as observed for rAP24NG usually suggest a conformational change, here associated with the interaction of the AP7 and AP24 polypeptide sequences, something that we do not see when glycosylation is present (i.e., rAP24G). This two-stage kinetic interaction can be observed more clearly by plotting the energy dissipation response against the resonant frequency for a given overtone, as shown in Figure 3. As noted on Figure 3, three distinct regions (i, ii, iii) can be observed due to interactions between rAP24NG and immobilized rAP7; (i) rAP24NG binding to the surface-immobilized rAP7 leading to a rapid increase in mass and viscoelasticity, (ii) a turning point where no more rAP24NG associates with rAP7, (iii) a reduction in mass and viscoelasticity that occurs over 30 minutes. We

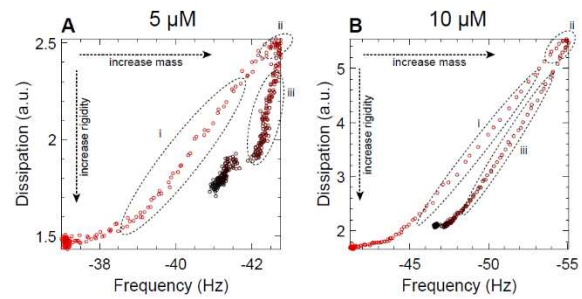


Figure 3. Interaction between surface-immobilized 5 μ M rAP7 with rAP24NG at 5 μ M (A) and 10 μ M (B). Changes in frequency and dissipation for the 7th overtone measured during interactions between rAP7 and rAP24NG at the aforementioned concentrations indicate a three-state interaction where (i) the complex gains mass and loses rigidity, (ii) complex restructures and (iii) trapped water and excess rAP24NG leaves surface. Increase in color darkness indicates time progression.

believe region (iii) is associated with a phase change where a critical concentration of associated rAP24NG results in hydrogel formation, leading to a loss in mass due to release of trapped water and excess rAP24NG.

Having confirmed interactions and kinetics between rAP7, rAP24G, and rAP24NG, and given that all individual proteins exhibit hydrogel formation in the presence of Ca(II),^{13,15} we next investigated whether or not glycosylation changes the outcome of co-hydrogel formation. We achieved this using flow cytometry,^{9,11,19} which probes the particle size distributions and internal granularities of the translucent protein hydrogel particles. Flow cytometry provides light scattering parameters that one can monitor for particles under constant flow:^{9,11,19} 1) Forward Scattered Component (FSC, x-axis), which determines particle size distributions; and 2) Side-Scattered Component (SSC, y-axis), measures refracted and reflected light that occurs at any interface within the particles where there is a change in refractive index (RI) that results from variations in particle granularity or internal structure (see Supporting Information). As shown in Figure 4, at pH 8.0 in the presence of Ca(II) rAP7

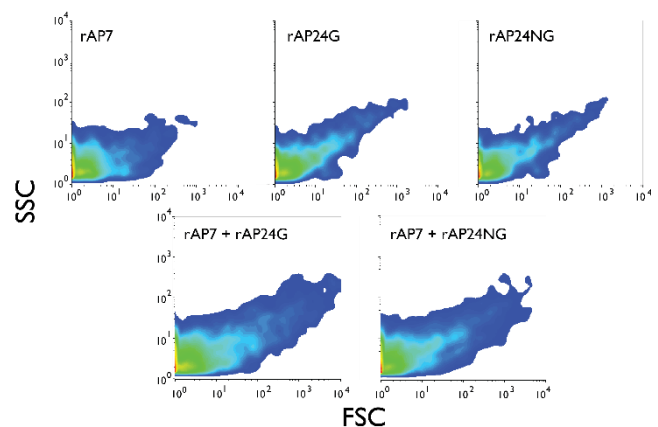


Figure 4. Flow cytometry 2-D density plots (FSC vs. SSC) of 1.5 μ M rAP7, rAP24G, rAP24NG, 1:1 rAP7 : rAP24G, 1:1 rAP7 : rAP24NG samples in 10 mM HEPES, 10 mM CaCl₂ pH 8.0. In the case of 1:1 molar mixtures the total protein concentrations are 1.5 μ M. Details regarding FSC and SSC parameters and other features can be found in Supporting Information.

forms hydrogel particles with unique particle size distributions and internal granularities compared to either rAP24G or rAP24NG. In comparison, rAP24G and rAP24NG both generate hydrogel particles that are somewhat similar in both physical categories. However, when present in a 1:1 mixture, we note an interesting effect: the rAP7 + rAP24G and rAP7 + rAP24NG samples generate 2-D density plots that differ from either rAP7, rAP24G, or rAP24NG individually. Thus, the resulting hydrogel particles formed by rAP7, rAP24G, and rAP24NG possess physical properties that are significantly different from hydrogel particles formed by the individual proteins, i.e., these are *hybrid* hydrogel particles. However, we note that the 2D plots for hydrogel particles generated in the rAP7 + rAP24G and rAP7 + rAP24NG samples are similar to one another except at the extreme ranges of particle size distributions and internal granularities. This result suggests that the majority of hydrogel complexes formed by either rAP7 + rAP24G or rAP7 + rAP24NG are dimensionally and internally similar to one another, and thus we believe that the glycan groups of rAP24G have very little impact on the resultant physical properties of the hybrid AP7 - AP24 protein hydrogel particles.

In this report, using model recombinant variants of *H. rufescens* AP7 and AP24, we confirm the 1:1 interactivity between these two nacre matrix protein sequences (Figure 2)¹⁷ and demonstrate the formation of hybrid hydrogel particles formed by these heteroprotein complexes (Figure 4). Thus, both AP7 and AP24 must co-exist together within the inclusions that make up the intracrystalline nanoporosities of the nacre of *H. rufescens*.¹⁷ In addition, the most interesting finding of this report are the complex effects of glycosylation, primary sequence, and Ca(II) on AP24 - AP7 interactions. As shown in Figure 1 and Figure S2 (Supporting Information) the glycan groups clearly enhance AP24G - AP7 adsorption. Yet, there is more to this story: when the glycan groups are absent, AP24 - AP7 binding still occurs but requires Ca(II) participation and proceeds with different kinetics and a conformational change event taking place within the AP24 sequence (Figures 1-3). Yet despite these kinetic differences, there is no significant difference in the physical character of the hybrid hydrogel complexes that form (Figure 4). Based upon these results, we surmise that the glycosylation of AP24 somehow enhances interactions with AP7 (Figure 1) but suppresses internal rearrangements within the AP24 sequence and shifts the kinetics of AP24 - AP7 binding. Surprisingly, glycosylation is not a pre-requisite for successful hybrid hydrogel formation (Figure 4). We interpret this to mean that if for some reason cellular errors occurred in the post-translational modification of AP24, these errors would not be fatal to AP7 - AP24 complex formation or *H. rufescens* nacre development. Thus, a "fail-safe" may be built into the AP7-AP24 relationship.¹⁷

Although we do not know what type of conformational change occurs within AP24 upon interaction with AP7, we do know that both proteins feature intrinsically disordered sequences,^{13,15} and it is known that these sequences can either undergo disorder-to-order conformational change upon protein-protein interaction, or, remain disordered until interaction with an appropriate target occurs later on.²⁰⁻²² Based upon this, we hypothesize that the glycan groups somehow allow AP24 - AP7 interactions to proceed but prevent a disorder-to-order transition within the AP24 sequence, possibly to allow AP24 to interact at another time with another target. Potential

"targets" could be other nacre layer proteins (e.g., AP8 series)^{17,18} or perhaps a mineral phase component. This is an intriguing and exciting possibility for the nacre biomineralization process and obviously additional studies involving protein fragments will be required to pinpoint the binding sites on each protein. Similarly, experiments involving other nacre proteins and calcium carbonate mineral phases will help to identify other potential targets that the AP7 - AP24 complex might interact with.

The present findings are in clear contrast to our earlier studies of another interactive pair of calcium-carbonate associated biomineralization matrix proteins, SpSM50 and rSpSM30B/C, from the embryonic spicules of the sea urchin *Strongylocentrotus pupuratus*.^{19,23-25} Here, the following was noted: 1) the glycan groups of the glycoprotein SpSM30B/C were required for interaction with SpSM50; 2) there was no noted interaction between the protein sequences themselves; 3) the hydrogel particles formed by glycosylated SpSM30B/C + SpSM50 were significantly different from those formed by unglycosylated SpSM30B/C + SpSM50. If we compare the AP7 + AP24 versus SpSM50 + SpSM30B/C interactions, we come to the following conclusions: a) glycosylation provides biomineralizing organisms an extra degree of control over protein-protein interaction and matrix assembly, either by modulating interactions or affinities between proteins or making them dependent upon other species, such as Ca(II), to foster matrix assembly. B) the glycosylation process can be tweaked by individual organisms to influence protein-protein interaction, matrix assembly, and mineral formation for the generation of a specific skeletal element. Hopefully, additional experimentation will determine if these hypothesis are correct.

ASSOCIATED CONTENT

Supporting Information

Detailed experimental procedures; discussion of FSC and SSC flow cytometry terms; details of rAP24G glycans; the primary amino acid sequences of AP7 and AP24 (Figure S1); Full QCM-D measurements of immobilized rAP7 exposed to either rAP24G or rAP24NG in 10 mM HEPES, pH 8.0 (Figure S2). The Supporting Information is available free of charge on the ACS Publications website as a PDF file.

AUTHOR INFORMATION

Yong Seob Jung ysj238@nyu.edu

Dr. John Spencer Evans jse1@nyu.edu

Jose-Juan Colas jose.juancolas@york.ac.uk

Steven Johnson steven.johnson@york.ac.uk

Corresponding Author

*To whom correspondence should be addressed. Tel: 347-753-1955; email jse1@nyu.edu

Author Contributions

The manuscript was written through contributions of all authors, and all authors have given approval to the final version of the manuscript.

Funding Sources

Portions of this research were supported by the Life Sciences Division, U.S. Army Research Office, under award W911NF-16-1-0262 (JSE). Research involving QCM-D measurements was supported by grants from the UK Engineering and Physical Sciences Research Council (EP/M02757/1, EP/P030017/1)(JJC, SJ)

Notes

The authors declare no competing financial interests.

ACKNOWLEDGMENT

This paper represents Contribution Number 98 from the Laboratory for Chemical Physics, New York University.

ABBREVIATIONS

AP7 = *H. rufescens* aragonite protein 7; AP24 = *H. rufescens* aragonite protein 24; rAP7 = recombinant AP7; rAP24G = insect cell glycosylated recombinant AP24; rAP24NG = bacteria-produced recombinant AP24, unglycosylated; QCM-D = quartz crystal microbalance with dissipation monitoring; ACC = amorphous calcium carbonate; FSC = forward scattered component; SSC = side scattered component; SpSM50 = *Strongylocentrotus purpuratus* spicule matrix protein 50; SpSM30B/C = *Strongylocentrotus purpuratus* spicule matrix protein 30, B/C hybrid variant.

ACCESSION ID:

AP7: GenBank AAK00635.1

AP24: GenBank AAK00634.1

REFERENCES

- 1 Studart, A.R. (2012) Towards high-performance bioinspired composites. *Adv. Materials* 24, 5024-5044.
- 2 Liu, X., Li, J., Xiang, L., Sun, J., Zheng, G., Zhang, G., Wang, H., Xie, L., Zhang, R. (2012) The role of matrix proteins in the control of nacreous layer deposition during pearl formation. *Proc. R. Soc. B* 279, 1000-1007.
- 3 Zhang, G., Fang, X., Guo, X., Li, L., Luo, R., Xu, F., Yang, P., Zhang, L., Wang, X., Qi, H., Xiong, Z., Que, H., Xie, Y., Holland, P.W.H., Wang, X., Paps, J., Zhu, Y., Wu, F., Chen, Y., Wang, J., Peng, C., Meng, J., Yang, L., Liu, J., Wen, B., Zhang, N., Huang, Z., Zhu, Q., Feng, Y., Mount, A., Hedgecock, D., Xu, Z., Liu, Y., Domazet-Lozo, T., Du, Y., Sun, X., Zhang, S., Liu, B., Cheng, P., Jiang, X., Li, J., Fan, D., Wang, W., Fu, W., Wang, T., Wang, B., Zhang, J., Peng, Z., Li, Y., Li, N., Wang, J., Chen, M., He, Y., Tan, F., Song, X., Zheng, Q., Huang, R., Yang, H., Du, X., Chen, L., Yang, M., Gaffney, P.M., Wang, S., Luo, L., She, Z., Ming, Y., Huang, W., Zhang, S., Huang, B., Zhang, Y., Qu, T., Ni, P., Miao, G., Wang, W., Zhang, S., Haung, B., Zhang, Y., Qu, T., Ni, P., Miao, G., Wang, J., Wang, Q., Steinberg, C.E.W., Wang, H., Li, N., Qian, L., Zhang, G., Li, Y., Yang, H., Liu, X., Wang, J., Yin, Y., Wang, J., (2012) The oyster genome reveals stress adaptation and complexity of shell formation. *Nature* 490, 49-54.
- 4 Fang, D., Xu, G., Hu, Y., Pan, C., Xie, L., Zhang, R. (2011) Identification of genes directly involved in shell formation and their functions in pearl oyster, *Pinctada fucata*. *PLOS One* 6, 1-13.
- 5 Liu, J., Yang, D., Liu, S., Li, S., Xu, G., Zheng, G., Xie, L., Zhang, R. (2015) Microarray: a global analysis of biomineralization-related gene expression profiles during larval development in the pearl oyster, *Pinctada fucata*. *BMC Genomics* 16, 325-340.
- 6 Marie, B., Joubert, C., Tayale, A., Zanella-Cleon, I., Belliard, C., Piquemal, D., Cochennec-Laureau, N., Marin, F., Gueguen, Y., Montagnani, C. (2012) Different secretory repertoires control the biomineralization processes of prism and nacre deposition of the pearl oyster shell. *Proc. Natl. Acad. Sci USA* 109, 20986-20991.
- 7 Jain, G., Pendola, M., Huang, Y.C., Colas, J.J., Gebauer, D., Johnson, S., Evans, J.S. (2017) Functional prioritization and hydrogel regulation phenomena created by a combinatorial pearl-associated 2-protein biomineralization model system. *Biochemistry* 56, 3607-3618.
- 8 Chang, E.P., Roncal-Herrero, T., Morgan, T., Dunn, K.E., Rao, A., Kunitake, J.A.M.R., Lui, S., Bilton, M., Estroff, L.A., Kröger, R., Johnson, S., Cölfen, H., Evans, J.S. (2016) Synergistic biomineralization phenomena created by a nacre protein model system. *Biochemistry* 55, 2401-2410.
- 9 Jain, G., Pendola, M., Huang, Y.C., Gebauer, D., Koutsoumpeli, E., Johnson, S., Evans, J.S. (2018) Selective synergism created by interactive nacre framework-associated proteins possessing EGF and vWA motifs. Implications for mollusk shell formation. *Biochemistry* 57, 2657-2666.
- 10 Pendola, M., Evans, J.S. (2018) Insights into mollusk shell formation: Interlamellar and lamellar specific nacre protein hydrogels differ in ion interaction signatures. *J. Phys. Chem B* 122, 1161-1168.
- 11 Perovic, I., Davidyants, A., Evans, J.S. (2016) Aragonite-associated mollusk shell protein aggregates to form mesoscale "smart" hydrogels. *ACS Omega* 1, 886-896.
- 12 Pendola, M., Jain, G., Davidyants, A., Huang, Y.C., Gebauer, D., Evans, J.S. (2016) A nacre protein forms mesoscale hydrogels that "hijack" the biomineralization process within a seawater environment. *Cryst. Eng. Commun.* 18, 7675-7679.
- 13 Chang, E.P., Perovic, I., Rao, A., Cölfen, H., Evans, J.S. (2016) Insect cell glycosylation and its impact on the functionality of a recombinant intracrystalline nacre protein, AP24. *Biochemistry* 55, 1024-1035.
- 14 Chang, E.P., Evans, J.S. (2015) Pif97, a von Willebrand and Peritrophin biomineralization protein, organizes mineral nanoparticles and creates intracrystalline nanochambers. *Biochemistry* 54, 5348-5355.
- 15 Perovic, I., Chang, E.P., Verch, A., Rao, A., Cölfen, H., Kroeger, R., Evans, J.S. (2014) An oligomeric C-RING nacre protein influences pre-nucleation events and organizes mineral nanoparticles. *Biochemistry* 53, 7259-7268.
- 16 Evans, J.S. (2013) "Liquid-like" biomineralization protein assemblies: A key to the regulation of non-classical nucleation. *Crystal Engineering Communications* 15, 8388 - 8394.
- 17 Michenfelder, M, Fu, G, Lawrence, C, Weaver, JC, Wustman, BA, Taranto, L, Evans, JS (2003) Characterization of two molluscan crystal-modulating biomineralization proteins and identification of putative mineral binding domains. *Biopolymers* 70, 522-533; errata 73: 522.
- 18 Fu G, Valiyaveetil, S., Wopenka, B., Morse, D.E. (2005) CaCO₃ biomineralization: acidic 8-kDa proteins from aragonitic abalone shell nacre can specifically modify calcite crystal morphology. *Biomacromolecules* 6, 1289-1298.

19 Jain, G., Pendola, M., Koutsoumpeli, E.W., Johnson, S., Evans, J.S. (2018) Glycosylation fosters interactions between model sea urchin spicule matrix proteins. Implications for embryonic spiculogenesis and biomineralization. *Biochemistry* 57, 3032-3035.

20 van der Lee, R., Buljan, M., Lang, B., Weatheritt, R.J., Daughdrill, G.W., Dunker, A.K., Fuxreiter, M., Gough, J., Gsponer, J., Jones, D.T., Kim, P.M., Kriwacki, R.W., Oldfield, C.J., Pappu, R.H., Tompa, P., Uversky, V.N., Wright, P.E., Babu, M.M. (2014) Classification of intrinsically disordered regions and proteins. *Chem. Rev.* 114, 6589-6631.

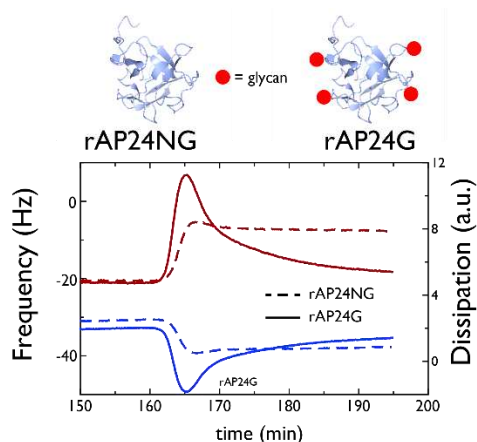
21 Uversky, V.N., Dunker, A.K. (2011) Multiparametric analysis of intrinsically disordered proteins: Looking at intrinsic disorder through compound eyes. *Anal. Chem.* 84, 2096-2104.

22 Ward, J.J., Sodhi, J.S., McGuffin, L.J., Buxton, B.F., Jones, D.T. (2004) Prediction and functional analysis of native disorder in proteins from the three kingdoms of life. *J. Mol. Biol.* 337, 635-645.

23 Pendola, M., Davidyants, A., Jung, Y.S., Evans, J.S. (2017) Sea urchin spicule matrix proteins form mesoscale hydrogels that exhibit selective ion interactions. *ACS Omega* 2, 6151-6158.

24 Jain, G., Pendola, M., Huang, Y.C., Gebauer, D., Evans, J.S. (2017) A model sea urchin spicule matrix protein, rSpSM50, is a hydrogelator that modifies and organizes the mineralization process. *Biochemistry* 56, 2663-2675.

25 Jain, G., Pendola, M., Rao, A., Cölfen, H., Evans, J.S. (2016) A model sea urchin spicule matrix protein self-associates to form mineral-modifying protein hydrogels. *Biochemistry* 55, 4410-4421.



For Table of Contents use only